ARCHIVES OF ELECTRICAL ENGINEERING VOL. 67(2), pp. 247–261 (2018)

DOI 10.24425/119638

A power constraint index to rank and group critical contingencies based on sensitivity factors

OSWALDO ARENAS-CRESPO, JOHN E. CANDELO

Facultad de Minas, Departamento de Energía Eléctrica y Automática
Universidad Nacional de Colombia, Sede Medellín
Carrera 80 No. 65-223, Medellín, Colombia
e-mail: oarenasc@unal.edu.co, jecandelob@unal.edu.co

(Received: 15.06.2017, revised: 15.01.2018)

Abstract: Finding the most critical contingencies in a power system is a difficult task as multiple evaluations of load and generation scenarios are needed. This paper presents a mathematical formulation for selecting, ranking, and grouping the most critical N-1 network contingencies, based on the calculation of a Power Constraint Index (PCI) obtained from the Outage Transfer Distribution Factors (OTDF). The results show that the PCI is only affected by the impedance parameter of the transmission network, the topology, and the location of all generators. Other methods, such as the Performance Index (PI) and the Overload Index (OL) are affected by the power generation and demand variations. The proposed mathematical formulation can be useful to accelerate the calculation of other methods that evaluate contingencies in power system planning and operation. Furthermore, the fast calculation of indices makes it suitable for online evaluation and classification of multiple events considering the current topology. The results showed that the proposed algorithm easily selected and ranked the expected contingencies, with the highest values of the index corresponding to the most critical events. In the filtering process, the computational calculation time improved without losing the robustness of the results.

Key words: contingency ranking, critical contingencies, power system operation, power system planning, sensitivity power factors

1. Introduction

The selection of critical contingencies is an important issue in transmission network planning and operation. A number of network planning applications must consider reliability and security studies with regard to different network element outages. Additionally, some online operation tools must monitor the state of the power grid by using indices obtained from contingency studies. However, the power generation, demand, and the topology can change, creating several scenarios to be considered in such studies.

www.czasopisma.pan.pl PAN POLSKA AKADEMIA NAUK www.journals.pan.pl

Therefore, finding the most critical contingencies for these different operation scenarios requires a significant amount of computation time. To simplify this task, some authors prefer to remove a number of low impact contingencies and only focus on critical events to appropriately monitor power system security [1, 2]. Furthermore, critical contingencies for online applications require a significant reduction in calculation time [3–5].

The main problem is the lack of an accurate mathematical model and the significant amount of information to be handled. As a result, many authors have proposed using artificial intelligence (AI) to rank and select critical contingencies [6–8]. Some of the analytical methods employed to rank contingencies consider the PI [8, 9] and OL [10, 11]. The PI finds a scalar that calculates the severity of a contingency based on the sum of the weighted deviations of power transfer through all elements of a power grid [13]. The OL index represents the current capability margin of power system elements, which is the actual state of the current flow with respect to the maximum current flow of an element.

The problem with these conventional methods is that the results are influenced by the specific operating point (demand and dispatch), requiring the simulation of many operation scenarios with different variations of power generation and demand. This affects the selection and ranking methods because, whereas a particular contingency may be critical in a specific scenario, in another scenario, the same contingency may not be critical; this implies that many scenarios need to be evaluated to provide a better ranking of critical contingency. Furthermore, these conventional and analytical techniques consume a significant amount of time and computational resources.

The present paper proposes a simple formulation called the PCI vector to select and rank critical network contingencies, and optionally group them by their impact on generation. This vector is composed of two indices obtained from the OTDF, called the Power Transfer Distribution Factor (PTDF) and the Line Outage Distribution Factor (LODF) [13, 14]. The proposed PCI vector considers only the network parameters and nonspecific operating scenarios needed to obtain the critical contingencies. Unlike most of the established methods, this method provides a list of ranked contingencies, with information of the element affected after each event, the overloaded element, and the participant generator. The relevant contribution of the proposed method is that the grouped constraints are not affected by variations in power generation and demand. The aim of using the PCI vector is to accelerate the calculation of different power system analysis methods, especially those used for network planning and operation. This method allows one to easily evaluate the critical contingencies as the topology changes, which is commonly needed for online operation.

2. Methodology

Fig. 1 presents the steps of the proposed method to select, rank, and group the $N-1$ network contingencies in the power system. In this figure, we have defined the inputs, the process to obtain the PCI vector, and the outputs that show the lists of the most critical contingencies. Next, we present a complete explanation of the process and the relevant mathematical formulas. This part of the algorithm performs all the processes necessary to calculate the final PCI vector, which obtains the critical contingencies grouped by generators.

2.1. Network implementation

In this first step (Fig. 1 – P1), we model the network and load the parameters required for studying each power system. In this step, we also consider all the possible scenarios that will help evaluate the proposed method's compliance with the main objective of this research. As an input, this step requires the definition of the network models and the parameters that will be used in each model (Fig. 1 – I1). For this research, we used two test cases: the IEEE 39-bus and the Colombian Atlantic power systems.

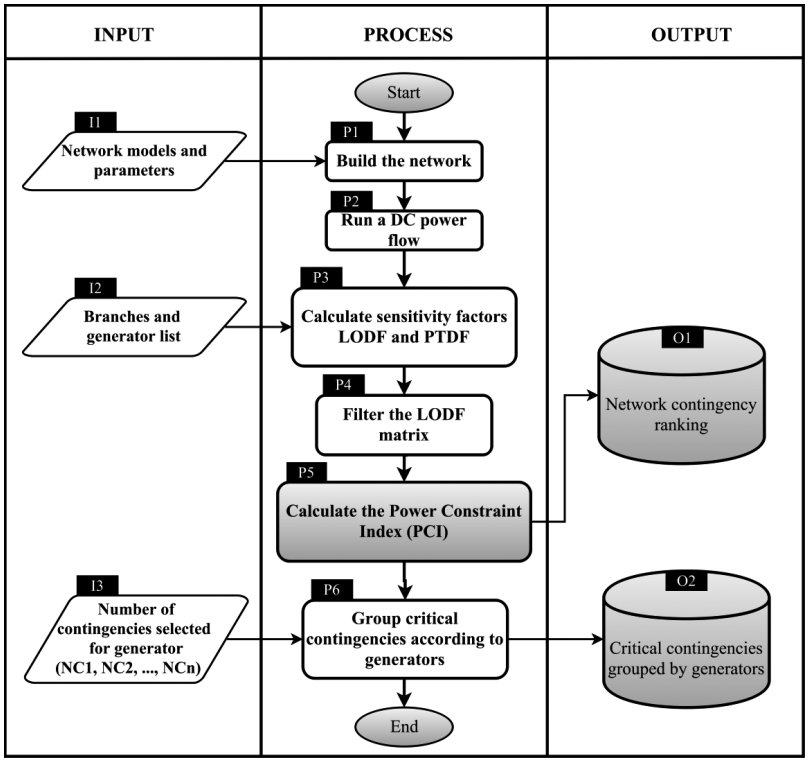

Fig. 1. Methodology to select, rank, and easily group the $N-1$ contingencies in a power system

2.2. DC power flow

A simple DC power flow is useful to determine the operating point of the power system (Fig. 1 – P2). The formulation of the DC power flow is shown in (1):

$$P_{km} = B_{km}\,\theta_{km}\,, \tag{1}$$

where P_{km} is the real power calculated with the DC power flow, B_{km} is the series susceptance of the line, and θ_{km} is the voltage angle difference between the buses k and m. In this approximation, the power flow is a function of the susceptance and the angle difference. At this step of the procedure, we run a DC power flow and all the results of the base case are used in the procedure, including the initial power through the branches.

www.czasopisma.pan.pl PAN POLSKA AKADEMIA NAUK www.journals.pan.pl

2.3. Sensitivity factors

To calculate the initial sensitivity factors (Fig. 1 – P3), we use the initial input parameters (Fig. 1 – I1). Then, we select only those branches and buses that can be considered as part of the network contingency study (Fig. 1 – I2). At this point, we only need to consider the linear operating condition to apply to the superposition theorem. Fig. 2 shows two diagrams that represent the power flow through two different lines before and after network contingencies. Starting from an initial operating point, we can monitor power flow P_i across line i before contingencies as shown in Fig. 2a. After a contingency occurs in line j, a new power flow $P_i^{(j)}$ is transferred through line i as shown in Fig. 2b.

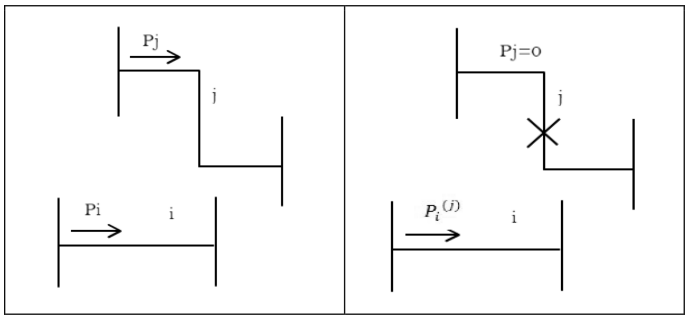

(a) (b)

Fig. 2. Power flow through two lines: (a) initial state; (b) after contingency of element j

The power variation in the lines with respect to a contingency can be represented by (2) [15, 16]:

$$P_i^{(j)} = P_i + \gamma_{ij} P_j \,, \tag{2}$$

where P_j is the power transfer in line j before the contingency, $P_i^{(j)}$ is the resulting power transfer in line i after the contingency of line j, and γ_{ij} is the LODF to monitor line i with respect to the outage of line j.

The values of γ_{ij} come from the partial derivate $(\partial P_i/\partial P_j)$, for which approximation is represented by $(\Delta P_i/\Delta P_j)$. This last expression describes linear behavior, which is a valid approximation for high voltage power transmission systems with a large X/R, small angles between buses, and voltage magnitudes near 1 pu (normal conditions for power system operation).

Similarly, it is possible to obtain the sensitivity factor that relates the power injection in bus k with the power flow by line i or line j as shown in Fig. 3.

The power variation in all lines of the network with respect to a power injection in bus k can be represented by (3). P_i is the initial power value in line i, P_k is the power injection in bus k, $P_i^{(k)}$ is the resulting power transfer to line i after the injection in bus k, and γ_{ik} is the PTDF of line i with respect to the power injection in bus k [15, 16]:

$$P_i^{(k)} = P_i + \gamma_{ik} P_k. \tag{3}$$

As for Equation (3), the PTDF for line j with respect to the power injection in bus k, is represented using (4). P_j is the initial power value in line j, P_k is the power injection in bus k,

www.czasopisma.pan.pl PAN POLSKA AKADEMIA NAUK www.journals.pan.pl

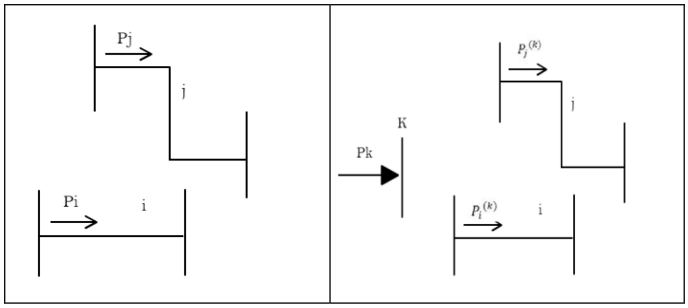

Fig. 3. Power flow through different lines: (a) initial state; (b) after contingency at bus k

$P_j^{(k)}$ is the resulting power transfer to line j after the injection in bus k, and γ_{jk} is the PTDF of line j with respect to the power injection in bus k [15, 16]:

$$P_j^{(k)} = P_j + \gamma_{jk} P_k \,. \tag{4}$$

From Equations (2), (3), and (4) we can obtain Expressions (5), (6), and (7):

$$\gamma_{ij} = \frac{P_i^{(j)} - P_i}{|P_j|} \,, \tag{5}$$

$$\gamma_{ik} = \frac{P_i^{(k)} - P_i}{|P_k|} \,, \tag{6}$$

$$\gamma_{jk} = \frac{P_j^{(k)} - P_j}{|P_k|} \,. \tag{7}$$

A sign correction is required in cases where the power value is negative (i.e. $P_i < 0$). Hence, the condition expressed in (4) can be considered to obtain the $[\gamma_{ij}]$ and the $[\gamma_{ik}]$ matrices from a power system:

$$\begin{aligned} P_i > 0; \;\; &\rightarrow \;\; \gamma_{ij} = \frac{P_i^{(j)} - P_i}{|P_j|} \,, \\ P_i < 0; \;\; &\rightarrow \;\; \gamma_{ij} = -\frac{P_i^{(j)} - P_i}{|P_j|} \,. \end{aligned} \tag{8}$$

With this correction, the γ_{ij} will have the following possible values:

- $\gamma_{ij} = 1$ represents the radial condition after a contingency or the radial topology between generation and element i.
- $\gamma_{ij} = -1$ represents the radial condition after a contingency or the case wherein the contingency is the same monitored element ($i = j$).
- $\gamma_{ij} > 0$ represents a power increase in element i after a contingency in element j.
- $\gamma_{ij} < 0$ represents a power decrease in element i. This result could also represent the change in the power flow direction in element i under the contingency in j.

www.czasopisma.pan.pl PAN POLSKA AKADEMIA NAUK www.journals.pan.pl

The expressions $[\gamma_{ij}]$ and $[\gamma_{ik}]$ are matrices created from the sensitivity factors of the network elements.

2.4. Filter the LODF matrix

The LODF matrix $[\gamma_{ij}]$ is rebuilt by deleting the rows with values lower than the parameter ρ provided as an input in the first step (Fig. 1 – I1). This parameter ρ is a real number that depends on the interconnections and topology of the power system. With this factor, we can filter the noncritical contingencies to reduce the number of cases to study and the computation time as shown in Fig. 1 (Fig. 1 – P4). This procedure results in a new matrix and this value will be used for calculating the PCI vector.

2.5. Calculate the PCI vector

This step in the procedure is the most important and the main contribution of this work. We consider the OTDF to determine the PCI vector (Fig. 1 – P5). Here, we considered the effect of both scenarios, the contingency in line j, and the power injection in bus k to obtain the expression shown in (9). This is the same expression shown in (2), but changes the initial power flow of elements i and j through the application of power injection into bus k. $P_i^{(jk)}$ represents the new power flow through element i once contingency j occurs and the power is injected in bus k as shown in Fig. 4:

$$P_i^{(jk)} = P_i^{(k)} + \gamma_{ij} P_j^{(k)} . \tag{9}$$

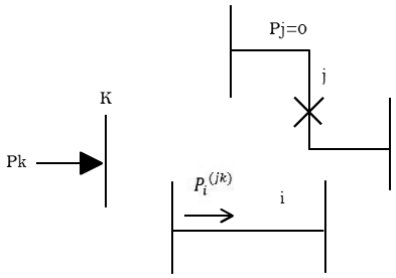

Fig. 4. Power flow $P_i^{(jk)}$ representation

On the other hand, with the value $P_i^{(jk)}$ calculated from the initial value of $P_i^{(j)}$ and with the superposition of power injection in bus k, we can obtain the equation shown in (10):

$$P_i^{(jk)} = P_i^{(j)} + P_k \psi , \tag{10}$$

where ψ is the OTDF that relates the effect of power injection into bus k, applying contingency j and monitoring the effect in element i. The ψ factor is not affected by the power system operation and depends only on the topology changes.

From (10), we can get the expression shown in (11):

$$\psi = \frac{P_i^{(jk)} - P_i^{(j)}}{P_k} . \tag{11}$$

Replacing (9) and (2) in (11), we obtained the expression shown in (12):

$$\psi = \frac{P_i^{(k)} + \gamma_{ij} P_j^{(k)} - (P_i + \gamma_{ij} P_j)}{P_k} . \tag{12}$$

Then, by replacing (3) and (4) in (12), the following expression for the OTDF ψ is obtained as shown in (13) [13, 14]:

$$\psi = \gamma_{ij}\, \gamma_{jk} + \gamma_{ik} . \tag{13}$$

Finally, if we add a weight that relates the maximum loading of each element, we can calculate the PCI vector using the formulation shown in (14). The PCI vector does not need a specific scenario to obtain the critical contingencies due to high correlation with the network parameters, which are not affected by the operation. In addition, the linear and short equations allow for the quick and easy calculation of all PCI:

$$PCI = (\gamma_{ij}\, \gamma_{jk} + \gamma_{ik}) * W_i , \tag{14}$$

where:

$$W_i = \frac{\min(P_{1-\max},\, P_{2-\max}, \ldots,\, P_{n-\max})}{P_{i-\max}} . \tag{15}$$

Factor W_i corresponds to the weight of a monitored element i ($i = 1, 2, \ldots n$), and is used to guarantee that the most severe cases of values in the PCI vector become higher than the less critical cases. $P_{1-\max}$, $P_{2-\max}$, ... and $P_{n-\max}$, are the maximum capacity of the lines, and $P_{i-\max}$ is the maximum power of a monitored element i.

Contingencies are ranked by the severity of the events, sorting from major to minor all values included in the PCI vector. The highest values represent the most critical contingencies in the network. When a monitored line obtains a high value of W_i, its power transfer capacity is lower than that of lines with lower values.

Fig. 5 shows the structure of the PCI vector obtained with (14). Each row of the PCI vector contains the analyzed contingency, the constrained elements that will be overloaded in some possible scenario, and the participant generator for the constraints. The contingency list output (Fig. 1 – O1) contains all the events simulated and ranked by the PCI. Note that each row gives more information on the constraints, representing an important advantage over other methods that relate only contingencies or overloaded elements.

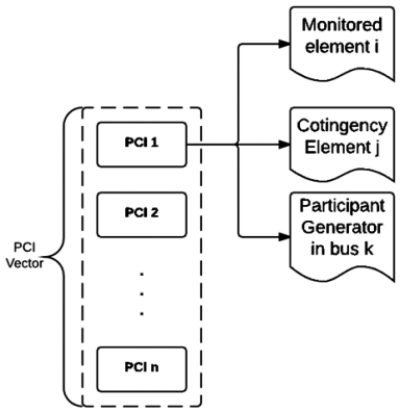

Fig. 5. General structure of the PCI vector

2.6. Grouping critical contingencies

Taking advantage of the results obtained in the PCI vectors, the critical network contingencies can be grouped by the generation effect. The aim of grouping contingencies by generators is to define the most critical events that can affect the power network operation. The maximum number of contingencies to show is provided as an input (Fig. 1 – I3) and a final critical contingency list calculated in (Fig. 1 – P6) is displayed in (Fig. 1 – O2). This final process avoids repeating the same participant generator more than the desired number of times for the constraints in the PCI vector, which represents low risk for the network operation.

3. Results and analysis

3.1. IEEE 39-bus power system test case

Fig. 6 shows the IEEE 39-bus power system test case, which is a simplified model of the New England power grid. This system has ten generators, wherein generator one is an equivalent representation of the rest of the power grid. This power system topology allows one to assess different power demand and generation dispatch scenarios.

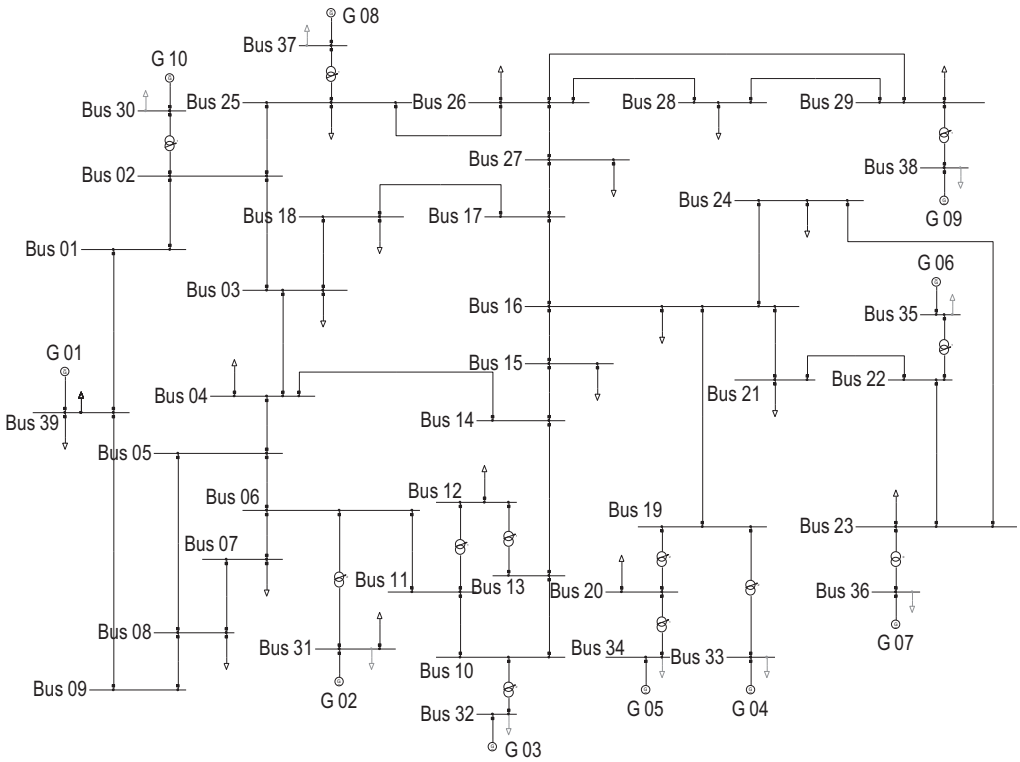

Fig. 6. IEEE 39-bus power system test case

3.1.1. Generation dispatches

Because the aim of this method is to identify the most critical contingencies of the network without the need to evaluate multiple dispatch and power load scenarios, we considered three different scenarios to compare the results with the PI and OL indices. The first scenario corresponds to the combination of the first dispatch shown in Table 1 and the current load of the power system. The second scenario corresponds to the second dispatch shown in Table 1, combined with the current load. Finally, the third scenario corresponds to the first dispatch shown in Table 1, but without loads.

Table 1. Generation dispatch for simulations

Generator	Dispatch 1 [MW]	Dispatch 2 [MW]
G 01	0	0
G 02	0	595
G 03	650	680
G 04	680	200
G 05	510	160
G 06	680	680
G 07	595	150
G 08	540	595
G 09	850	450
G 10	250	400

The first two scenarios were implemented to examine differences in the power flow through the element branches and the third scenario was proposed to demonstrate that the PCI vector can be calculated even in a non-convergence scenario because it only depends on the network parameter.

3.1.2. Power grid constraints

Table 2 presents the overloaded elements obtained after studying each contingency. These overloaded elements were found using an $N-1$ contingency analysis under the three scenarios

Table 2. Constraints identified from the two dispatches

Number	Contingency	Overload element
1	Line 21–22	Line 23–24
2	Line 10–11	Line 10–13
3	Line 15–16	Line 16–17
4	Line 01–02	Line 09–39
5	Line 08–09	Line 01–39
6	Line 16–17	Line 14–15
7	Line 10–13	Line 10–11
8	Line 23–24	Line 21–22
9	Line 04–14	Line 06–11
10	Line 06–11	Line 04–14
11	Line 14–15	Line 03–18
12	Line 02–03	Line 25–26
13	Line 13–14	Line 04–05
14	Line 04–05	Line 13–14

www.czasopisma.pan.pl PAN POLSKA AKADEMIA NAUK www.journals.pan.pl

previously described. With these contingencies, the PCI, PI, and OL are compared to identify the results according to the objective previously defined.

3.1.3. Contingency selection and ranking

Table 3 shows the results of the PCI, PI, and OL for the three proposed scenarios. The calculation of PCI was performed using a DC power flow and the PI and OL indices were calculated using an AC load flow.

Table 3. Comparison of the PCI results with other indices

	Scenario 1			Scenario 2			Scenario 3		
Cont.	**OL (%)**	**PI**	**PCI**	**OL (%)**	**PI**	**PCI**	**OL (%)**	**PI**	**PCI**
1	170	14.00	0.502	95	17.94	0.502	213	164.84	0.502
2	109	11.14	0.502	115	15.59	0.502	109	165.89	0.502
3	107	11.99	0.502	104	17.12	0.502	413	189.05	0.502
4	48	8.73	0.502	226	23.89	0.502	796	345.75	0.502
5	51	11.26	0.502	217	23.63	0.502	796	238.02	0.502
6	56	10.18	0.502	162	17.58	0.502	413	189.1	0.502
7	108	9.83	0.502	118	20.49	0.502	109	155.61	0.502
8	129	11.67	0.386	75	15.9	0.386	164	162.17	0.386
9	110	10.36	0.379	26	15.28	0.379	274	170.07	0.379
10	113	11.97	0.367	23	15.46	0.367	279	172.83	0.367
11	30	8.85	0.364	162	23.72	0.364	368	189.05	0.364
12	66	12.16	0.275	176	24.7	0.275	233	169.31	0.275
13	21	9.91	0.237	179	22.93	0.237	27	156.65	0.237
14	25	8.84	0.223	172	19.63	0.223	240	184.06	0.223

In this table, the values of the PCI vector remain constant for the different scenarios evaluated in the test. For example, constraint number 1 obtained a value of 0.502 for the three scenarios, showing that this is a stable method to identify critical contingencies. Other important characteristics of the PCI include the low variability from one constraint to another. This explains why constraints from one to seven have the same value.

When comparing these results with the PI and OL, the two final indices changed the values due to the variation of the constraints and the scenarios. For example, constraint number 4 is the most severe in scenario 2; however, in scenario 1 it has one of the lowest positions. Furthermore, the different values obtained with the PI and LO indices when changing scenarios show the difficulties in identifying the most critical network contingencies.

In a non-demand scenario, the AC load flow has no convergence, and we had to calculate the PI and OL with the DC power flow. Once again, the PCI index has the same values, even with all the power grid loads switched off. Instead of this, the PI and OL indices vary, confirming that the contingency analysis is affected by the power changes tested in this research.

Table 4 shows the contingencies grouped by their respective generators in the IEEE 39-bus power system test case. In this case, we have selected to show only one contingency for each power system generator.

The results obtained in Table 2 can be compared with the columns “Contingency” and “Element (j)” in Table 4. In these last results, contingency one (Line 21–22) is highly affected by

Table 4. Critical contingencies grouped by generator

PCI	Element (*i*)	Element (*j*)	Bus Gen. (*k*)	Position in PCI vector
0.502	Line 28–29	Line 26–29	Gen9	0
0.502	Line 26–27	Line 02–25	Gen8	6
0.502	Line 23–24	Line 22–23	Gen7	10
0.502	Line 23–24	Line 21–22	Gen6	12
0.502	Line 16–17	Line 15–16	Gen5	34
0.502	Line 16–17	Line 14–15	Gen4	39
0.502	Line 13–14	Line 06–11	Gen3	48
0.502	Line 09–39	Line 01–39	Gen2	58
0.502	Line 09–39	Line 01–02	Gen10	68

generator six and the element overloaded in many possible scenarios will be Line 23–24. Contingency three (Line 15–16) is highly affected by generator five, and one of the most overloaded elements in some of the possible scenarios is Line 16–17.

3.2. Colombian Atlantic power system test case

Fig. 7 shows the Colombian Atlantic power system test case. This power system is a simplification of an area of the Colombian Interconnected power system.

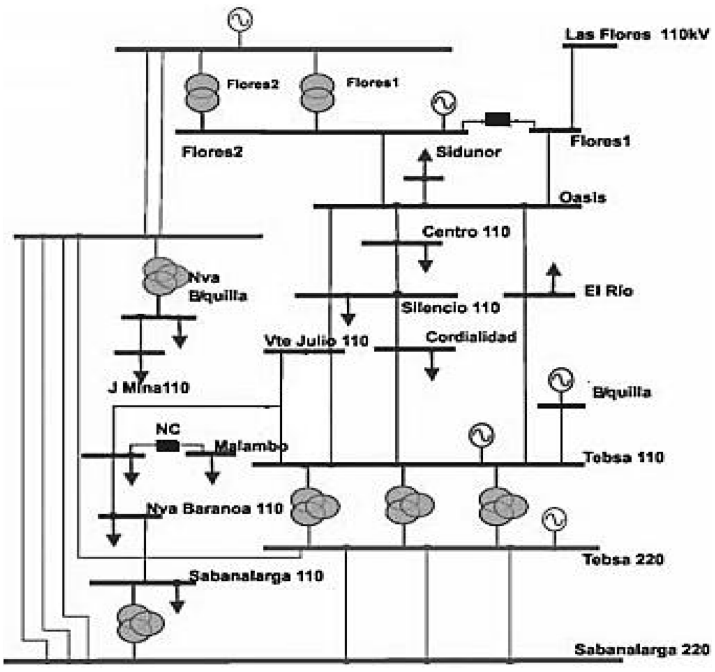

Fig. 7. Colombian Atlantic power system. Source: UPME [18]

www.czasopisma.pan.pl PAN POLSKA AKADEMIA NAUK www.journals.pan.pl

We selected this system to simulate other scenarios that can be presented in a real power system and show the advantages of the proposed method. The system has six generators, seven transformers, and forty-four lines. A generator was located in Sabanalarga, at 220 kV, which represents an equivalent network in the Colombian Interconnected power system as the slack bus. This network topology allows for the assessment of different power demand and generation dispatch scenarios.

3.2.1. Generation dispatches

Three generation dispatch scenarios were considered in this research to select the most critical contingencies. Table 5 shows two selected generation dispatches, representing an important variation in the power flow when the element outages are presented.

Table 5. Power generation dispatch

Generator	Dispatch 1 [MW]	Dispatch 2 [MW]
Flores 110	80	140
Flores 220	0	344
Barranquilla	110	55
Tebsa 110	184	92
Tebsa 220	607.04	257.42

The first scenario is composed of the original power demand and generation dispatch 1. The second scenario is composed of the current power demand and generation dispatch 2. Finally, the third scenario is composed of generation dispatch one with no load.

3.2.2. Power grid constraints

Table 6 presents the constraints calculated in the Colombian Atlantic power system test case.

Table 6. Constraints found in the Colombian Atlantic power system

No	Contingency	Overload Element
1	Oasis—Termoflores II 1 110	Oasis—Termoflores I 1 110
2	Oasis—Termoflores I 1 110	Oasis—Termoflores II 1 110
3	Flores 220/110 2	Oasis—Termoflores II 1 110
4	Flores—Nv Barranquilla 1 220	Flores—Nv Barranquilla 2 220
5	Oasis—Silencio 1 110	Centro—Oasis 1 110
6	Tebsa 3 214.5/110	Tebsa 2 220/110
7	Tebsa—Union 1 110	El Rio—Tebsa 1 110
8	Las Flores—Termoflores I 1 110	Oasis—Silencio 1 110
9	Tebsa—Vte Julio 1 110	TVte Julio—Vte Julio 1 110
10	Sabanalarga—Tebsa 3 220	Sabanalarga—Tebsa 1 220
11	Tebsa—TVte Julio 1 110	Tebsa—Vte Julio 1 110
12	Tebsa—Vte Julio 1 110	Tebsa—TVte Julio 1 110

www.czasopisma.pan.pl PAN POLSKA AKADEMIA NAUK www.journals.pan.pl

To find these constraints, we calculated the N-1 contingencies under the scenarios previously defined. Next, we searched for the highest overloaded elements in the power grid. Using these contingencies, we compared the results of the PCI, PI, and OL indices to show their behavior under different scenarios.

3.2.3. Contingency selection and ranking

Table 7 shows the calculation of PCI, PI, and OL under the three scenarios presented in the Colombian Atlantic power system test case. Similar to the results obtained with the first power system test case, the OL and PI vary according to each scenario, whereas the PCI maintains the same value. For example, the first contingency has the same value for all three scenarios. The same value also can be obtained for different contingencies, representing the critical events. These results show that the PCI is stable and that there is no need to consider a specific scenario to receive valid values.

Table 7. Contingency selection

Cont	Scenario 1			Scenario 2			Scenario 3 (DC)		
	OL (%)	PI	PCI	OL (%)	PI	PCI	OL (%)	PI	PCI
1	84.1	7.0	0.2	152.9	6.5	0.2	43.9	7.1	0.2
2	72.1	6.8	0.2	129.0	6.0	0.2	37.4	7.0	0.2
3	45.4	6.9	0.2	82.1	5.6	0.2	17.6	7.5	0.2
4	32.4	6.7	0.2	74.4	5.7	0.2	48.9	7.1	0.2
5	82.5	6.8	0.2	141.3	6.2	0.2	48.6	7.1	0.2
6	73.9	6.9	0.1	57.8	6.2	0.1	70.9	8.3	0.1
7	122.2	7.5	0.1	85.4	5.8	0.1	18.0	7.0	0.1
8	60.0	7.0	0.1	87.9	6.3	0.1	28.0	7.1	0.1
9	104.9	8.7	0.1	75.9	6.5	0.1	6.1	7.0	0.1
10	53.7	7.2	0.1	23.2	5.5	0.1	111	9.1	0.1
11	141.0	7.8	0.1	106.6	6.1	0.1	46.4	7.3	0.1
12	137.3	8.7	0.1	104.0	6.5	0.1	45.9	7.0	0.1

Table 8 shows the results of the contingencies grouped by each generator in the Atlantic power system test case. In this case, we have chosen to select only two contingencies for each generator.

Comparing Table 6 with Table 8 in the columns "Contingency" and "Elem(j)," we see that, for contingency number 1, the major incidence is Flores 110 and the overloaded element in many possible scenarios is Oasis—Termoflores II 1 110. For contingency 6, the generator with a major impact is TEBSA 110 and the element overloaded in many possible scenarios will be Tebsa 2 220/110.

www.czasopisma.pan.pl PAN POLSKA AKADEMIA NAUK www.journals.pan.pl

Table 8. Contingency grouping selection

PCI	Elem(*i*)	Elem(*j*)	BusGen(*k*)	Position in PCI vector
0.198	Oasis—Termoflores I 1 110	Oasis—Termoflores II 1 110	FLORES 110	0
0.1772	Oasis—Termoflores II 1 110	Oasis—Termoflores I 1 110	FLORES 110	1
0.1676	Flores—Nv Barranquilla 2 220	Flores—Nv Barranquilla 1 220	FLORES 220	4
0.1676	Flores—Nv Barranquilla 1 220	Flores—Nv Barranquilla 2 220	FLORES 220	5
0.1439	Tebsa 2 220/110	Tebsa 3 214.5/110	TEBSA 110	7
0.1332	Tebsa 3 214.5/110	Tebsa 2 220/110	TEBSA 110	16
0.0835	Sabanalarga—Tebsa 2 220	Sabanalarga—Tebsa 3 220	TEBSA 220	176
0.0834	Sabanalarga—Tebsa 2 220	Sabanalarga—Tebsa 1 220	TEBSA 220	178

4. Conclusions

This paper presented a simple formula for selecting the most critical $N-1$ network contingencies of a power system. The method is based on the application of PTDF and OTDF for calculating a simple mathematical expression called the PCI. The aim of this formulation is to classify and rank the network contingencies independently of power demand and generation variations. The results showed that the proposed algorithm easily selected and ranked the expected contingencies, with the highest values of the index corresponding to the most critical events. In the filtering process, the computational calculation time improved without losing the robustness of the results. A comparison with two conventional methods, PI and OL, showed that there is no need for the PCI to simulate all possible scenarios in the power system because it is directly related to the network parameters and the topology. The proposed method provides a significant contribution due to the fast generation of contingencies for online applications, which are different for power system planning and operation. In future work, we will work on using this method for new applications in power system operation and planning, and investigate its application in real-time operations.

References

[1] Morison K., Wang L., Kundur P., *Power system security assessment*, IEEE Power and Energy Magazine, vol. 2, no. 5, pp. 30–39 (2004), DOI: 10.1109/MPAE.2004.1338120.

[2] Stefopoulos G.K., Yang F., Cokkinides G.J., Meliopoulos A.P., *Advanced contingency selection methodology*, Proc. 37th Annual North Amaerican Power Symposium, IEEE; n.d., pp. 67–73 (2005), DOI: 10.1109/NAPS.2005.1560503.

[3] Gimenez Alvarez J.M., Mercado P.E., *Online Inference of the Dynamic Security Level of Power Systems Using Fuzzy Techniques*, IEEE Transactions on Power Systems, vol. 22, no. 2, pp. 717–726 (2007), DOI: 10.1109/TPWRS.2007.895161.

[4] Chen Y., Bose A., *Direct ranking for voltage contingency selection*, IEEE Transactions on Power Systems, vol. 4, no. 4, pp. 1335–1344, DOI: 10.1109/59.41683.

www.czasopisma.pan.pl PAN POLSKA AKADEMIA NAUK www.journals.pan.pl

[5] Morison K., Wang X., Moshref A., Edris A., *Identification of voltage control areas and reactive power reserve; An advancement in on-line voltage security assessment*, IEEE Power and Energy Society General Meeting – Conversion and Delivery of Electrical Energy in the 21st Century, Pittsburgh, PA, USA, pp. 1–7 (2008), DOI: 10.1109/PES.2008.4596339.

[6] McCalley J.D., Krause B.A., *Rapid transmission capacity margin determination for dynamic security assessment using artificial neural networks*, Electric Power Systems Research, vol. 34, no. 1, pp. 37–45 (1995), DOI: 10.1016/0378-7796(95)00955-H.

[7] Kezunovic M., Rikalo I., Sobajic D.J., *Real-Time and off-line transmission line fault classification using neural networks*, Engineering Intelligent Systems, vol. 4, no. 1, pp. 57–63 (1996).

[8] Ghosh S., Chowdhury B.H., *Design of an artificial neural network for fast line flow contingency ranking*, International Journal of Electrical Power and Energy Systems, vol. 18, no. 5, pp. 271–277 (1996), DOI: 10.1016/0142-0615(94)00021-2.

[9] Sekhar P., Mohanty S., *An online power system static security assessment module using multi-layer perceptron and radial basis function network*, International Journal of Electrical Power and Energy Systems, vol. 76, pp. 165–173 (2016), DOI: 10.1016/j.ijepes.2015.11.009.

[10] Gasim Mohamed S.E., Yousif Mohamed A., Abdelrahim Y.H., *Power System Contingency Analysis to detect Network Weaknesses*, Zaytoonah University International Engineering Conference on Design and Innovation in Infrastructure, Amman, Jordan, pp. 1–11 (2012).

[11] Fliscounakis S., Panciatici P., Capitanescu F., Wehenkel L., *Contingency Ranking With Respect to Overloads in Very Large Power Systems Taking Into Account Uncertainty, Preventive, and Corrective Actions*, IEEE Transactions on Power Systems, vol. 28, no. 4, pp. 4909–4917 (2013), DOI: 10.1109/TPWRS.2013.2251015.

[12] Majidi-Qadikolai M., Baldick R., *Integration of Contingency Analysis With Systematic Transmission Capacity Expansion Planning: ERCOT Case Study*, IEEE Transactions on Power Systems, vol. 31, no. 3, pp. 2234–2245 (2016), DOI: 10.1109/TPWRS.2015.2443101.

[13] Kumar Patra K., *Contingency Analysis in Power System using Load Flow Solution*, IEEE International Conference on Power Electronics, Intelligent Control and Energy Systems (ICPEICES), Delhi, India, pp. 1–4 (2016), DOI: 10.1109/ICPEICES.2016.7853352.

[14] Zhu J., *Optimization of Power System Operation*, New Jersey: John Wiley & Sons, Inc. (2009), DOI: 10.1002/9780470466971.

[15] Eastern Interconnection Reliability Assessment Group, *Study Procedure Manual* 2015.

[16] Chen Y.C., Dominguez-Garcia A.D., Sauer P.W., *Generalized injection shift factors and application to estimation of power flow transients*, North American Power Symposium, pp. 1–5 (2014), DOI: 10.1109/NAPS.2014.6965399.

[17] Guo J., Fu Y., Li Z., Shahidehpour M., *Direct Calculation of Line Outage Distribution Factors*, IEEE Transactions on Power Systems, vol. 24, no. 3, pp. 1633–1634 (2009), DOI: 10.1109/TPWRS.2009.2023273.

[18] Unidad de Planeación Minero Energética – UPME., *Plan de expansión de referencia generación-transmisión* 2014–2028, Bogotá, Colombia (2014).